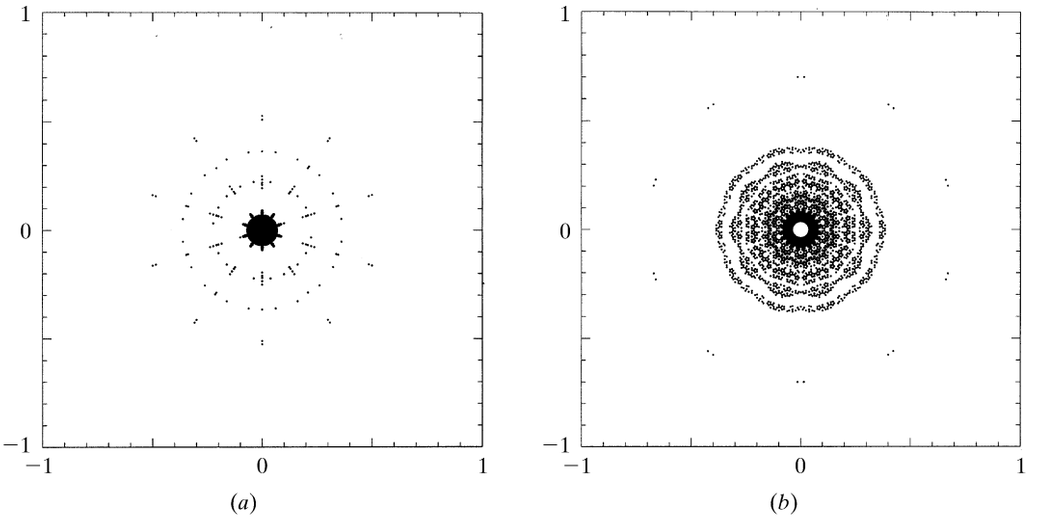

Fig. 4.6.3.37. Perpendicular-space distribution of (*a*) positive and (*b*) negative structure factors of the 3D Penrose tiling of the 6D *P* lattice type decorated with point atoms (edge lengths of the Penrose unit rhombohedra $a_r = 5.0$ Å). The magnitudes of the structure factors are indicated by the diameters of the filled circles. All reflections are shown within $10^{-4}|F(\mathbf{0})|^2 < |F(\mathbf{H})|^2 < |F(\mathbf{0})|^2$ and $-6 \le h_i \le 6, i = 1, \ldots, 6$.

4.6.4. Experimental aspects of the reciprocal-space analysis of aperiodic crystals

4.6.4.1. *Data-collection strategies*

Theoretically, aperiodic crystals show an infinite number of reflections within a given diffraction angle, contrary to periodic crystals. The number of reflections to be included in a structure analysis of a *periodic* crystal may be very high (one million for virus crystals, for instance) but there is no ambiguity in the selection of reflections to be collected: all Bragg reflections within a limiting sphere in reciprocal space, usually given by $0 \le \sin\theta/\lambda \le 0.7$ Å^{-1}, are used. All reflections, observed and unobserved, are included to fit a reliable structure model.

However, for *aperiodic* crystals it is not possible to collect the infinite number of dense Bragg reflections within $0 \le \sin\theta/\lambda \le 0.7$ Å^{-1}. The number of observable reflections within this limiting sphere depends only on the spatial and intensity resolution.

What happens if not all reflections are included in a structure analysis? How important is the contribution of reflections with large perpendicular-space components of the diffraction vector which are weak but densely distributed? These problems are illustrated using the example of the Fibonacci sequence. An infinite model structure consisting of Al atoms with isotropic thermal parameter $B = 1$ Å^2, and distances S $= 2.5$ Å and L $= \tau$ S, was used for the calculations (Table 4.6.4.1).

It turns out that 92.6% of the total diffracted intensity of 161 322 reflections is included in the 44 strongest reflections and 99.2% in the strongest 425 reflections. It is remarkable, however, that in all the experimental data for icosahedral and decagonal quasicrystals collected so far, rarely more than 20 to 50 reflections along reciprocal-lattice lines corresponding to net planes with Fibonacci-

Table 4.6.4.1. *Intensity statistics of the Fibonacci chain for a total of 161 322 reflections with* $-1000 \le h_i \le 1000$ *and* $0 \le \sin\theta/\lambda \le 2$ Å^{-1}

In the upper line, the number of reflections in the respective interval is given; in the lower line the partial sums $\sum I(\mathbf{H})$ of the intensities $I(\mathbf{H})$ are given as a percentage of the total diffracted intensity. The $F(00)$ reflection is not included in the sums.

	$F(\mathbf{H})/F(\mathbf{H})_{\max} \ge 0.1$	$0.1 > F(\mathbf{H})/F(\mathbf{H})_{\max} \ge 0.01$	$0.01 > F(\mathbf{H})/F(\mathbf{H})_{\max} \ge 0.001$	$F(\mathbf{H})/F(\mathbf{H})_{\max} < 0.001$
$0 \le \sin\theta/\lambda \le 0.2$ Å^{-1}	17	148	1505	14 511
$\sum I(\mathbf{H})$	52.53%	2.56%	0.27%	0.03%
$0.2 \le \sin\theta/\lambda \le 0.4$ Å^{-1}	11	107	1066	14 998
$\sum I(\mathbf{H})$	27.03%	2.03%	0.19%	0.02%
$0.4 \le \sin\theta/\lambda \le 0.6$ Å^{-1}	9	64	654	15 456
$\sum I(\mathbf{H})$	9.84%	0.96%	0.12%	0.01%
$0.6 \le \sin\theta/\lambda \le 0.8$ Å^{-1}	6	27	326	15 823
$\sum I(\mathbf{H})$	2.94%	0.34%	0.07%	0.01%
$0.8 \le \sin\theta/\lambda \le 2$ Å^{-1}	1	35	338	96 720
$\sum I(\mathbf{H})$	0.23%	0.79%	0.06%	0.01%
Total sum	44	381	3389	157 508
	92.57%	6.67%	0.70%	0.06%

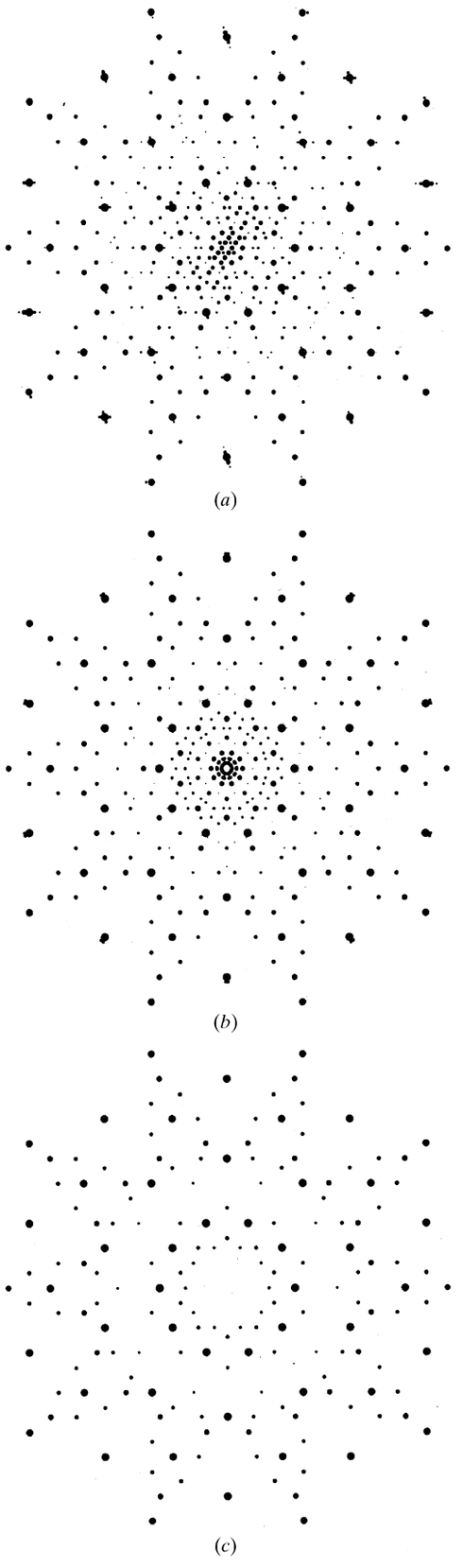

Fig. 4.6.4.1. Simulated diffraction patterns of (*a*) the $\simeq 52$ Å single-crystal approximant of decagonal Al–Co–Ni, (*b*) the fivefold twinned approximant, and (*c*) the decagonal phase itself (Estermann *et al.*, 1994).

sequence-like distances could be observed. The consequences for structure determinations with such truncated data sets are primarily a lower resolution in perpendicular space than in physical space. This corresponds to a smearing of the hyperatoms in the perpendicular space. For the derivation of the local structure-building elements (clusters) of aperiodic crystals this is only a minor problem: the smeared hyperatoms give rise to split atoms and a biased electron-density distribution. The information on the global aperiodic structure, however, which is contained in the detailed shape of the atomic surfaces, is severely reduced when using a low-resolution diffraction data set. A combination of high-resolution electron microscopy, lattice imaging and diffraction techniques allows a good characterization of the local and global order even in these cases. For a more detailed analysis of these problems see Steurer (1995).

4.6.4.2. *Commensurability versus incommensurability*

The question whether an aperiodic crystal is really aperiodic or rather a high-order approximant is of different importance depending on the point of view. As far as real finite crystals are considered, definitions of *periodic* and *aperiodic real crystals* and of *periodic* and *aperiodic perfect crystals* have to be given first. *Real crystals*, despite periodicity or aperiodicity, are the actual samples under investigation. Partial information about their actual structure can be obtained today by imaging methods (scanning tunnelling microscopy, atomic force microscopy, high-resolution transmission electron microscopy, . . .). Basically, the real crystal structure can be determined using full diffraction information from Bragg and diffuse scattering. In practice, however, only 'Bragg reflections' are included in a structure analysis. 'Bragg reflections' result from the integration of diffraction intensities from extended volumes around a limited number of Bragg-reflection positions ($\mathbb{Z}$ module). This process of intensity condensation at Bragg points corresponds in direct space to an averaging process. The real crystal structure is projected upon one unit cell in direct space defined by the $\mathbb{Z}$ module in reciprocal space. Generally, the identification of appropriate reciprocal-space metrics is not a problem in the case of crystals. It can be problematic, however, in the case of aperiodic crystals, in particular quasicrystals (see Lancon *et al.*, 1994). The metrics, and to some extent the global order in the case of quasicrystals, are fixed by assigning the reciprocal basis. The spatial resolution of a diffraction experiment defines the accuracy of the resulting metrics. The decision whether the rational number obtained for the relative length of a satellite vector indicates a commensurate or an incommensurate modulation can only be made considering temperature- and pressure-dependent chemical and physical properties of the material. The same is valid for other types of aperiodic crystals.

4.6.4.3. *Twinning and nanodomain structures*

High-order approximants of quasicrystals often occur in orientationally twinned form or, on a smaller scale, as oriented nanodomain structures. These structures can be identified by electron microscopy, and, in certain cases, also by high-resolution X-ray diffractometry (Kalning *et al.*, 1994). If the intensity and spatial resolution is sufficient, characteristic reflection splitting and diffuse diffraction phenomena can be observed. It has been demonstrated that for the determination of the local structure (structure-building elements) it does not matter greatly whether one uses a data set for a real quasicrystal or one for a twinned approximant (Estermann *et al.*, 1994). Examples of reciprocal-space images of an approximant, a twinned approximant and the related decagonal phase are shown schematically in Fig. 4.6.4.1 and for real samples in Fig. 4.6.4.2.

references